

Consensus Based Formation Control for Multi-UAV Systems with Time-varying Delays and Jointly Connected Topologies*

Tianyi Xiong, Zhiqiang Pu, Jianqiang Yi, *Senior Member, IEEE*, and Xinlong Tao

Abstract—This paper investigates the time-varying formation control problem for multiple unmanned aerial vehicle (multi-UAV) systems with time-varying delays and jointly connected topologies. Firstly, a consensus based formation control law is proposed to realize and maintain the desired time-varying formation in presence of time-varying delays and jointly connected topologies. Then, a sufficient condition in terms of linear matrix inequalities (LMI) is derived for formation control and the stability of the close-loop system is analyzed by employing Lyapunov-Krasovskii function. Finally, two task-oriented formation transformation cases are simulated to verify the effectiveness of the proposed control law, where the first is to shape varying regular hexagon, and the second is to avoid multiple obstacles.

I. INTRODUCTION

Recently, formation flight for multiple unmanned aerial vehicle (multi-UAV) systems has received significant attention from both researchers and engineers, due to its outstanding advantages including wide area sensing coverage, low cost, good flexibility performance, strong robustness to system failure, and so on. Generally, the primary research concern in formation flight is to shape and stabilize the expected formations for multi-UAV systems by means of effective control methods. Consequently, considerable efforts in formation control have been made. Three typical strategies, namely, leader-follower based approach [1], behavior based method [2], and virtual structure based strategy [3], have been proposed and studied for formation control.

However, it should be pointed out these three typical strategies have their own weaknesses [4]. Over the past several years, great development in consensus theory for multi-agent systems has been achieved, and increasing results based on consensus theory have been derived to deal with formation control problem. Through introducing a distributed finite-time observer based on consensus theory, a finite-time formation control was obtained for a group of nonholonomic mobile robots in [5]. Distributed invariant formation control problem for multi-UAV systems have been investigated in presence of time-varying delays and switching topologies in [6]. However, it should be pointed out that all of the formations in the results above are time-invariant, which often cannot satisfy various practical requirements. Therefore, it motivates some researches on time-varying formation control. Time-varying formation tracking control problem for multiple manipulators in finite time was studied in [7]. Under switching interaction topologies, the same problem for second-order

multi-agent systems has been investigated in [8], where the obtained results were applied to deal with the target enclosing problem for a multi-quadrotor system.

As we all know, time delays are inevitable in reality during information exchanging, which can severely influence the formation control performance. Thus, it is meaningful to investigate formation control problems with time delays. Ref. [9] investigated a leader-following formation control problem for multi-agent systems with non-uniform time-varying communication delays. Ref. [10] proposed a consensus based algorithm to solve formation control problems for multiple unmanned underwater vehicles with time-varying delays.

Besides, communication failures or new creations of communication links may occur in practice. In these cases, the interactions among UAVs will change, which results in a great significance to take switching communication topologies into consideration in formation control. Time-varying formation control for linear multi-agent systems under switching directed topologies was studied in [11]. Time-varying formation control for multi-UAV systems with switching connected topologies was investigated in [12].

Nevertheless, to the best of our knowledge, there are few results available to simultaneously solve time-varying delays and switching topologies problems for time-varying flight formation control, which motivates this study. Ref. [6] took both time-varying delays and switching topologies into consideration in the formation control for multi-UAV systems, but the desired formation was invariant. Ref. [13] proposed a distributed time-varying formation control law for multi-UAV systems with time delays. However, switching topologies were not considered in this paper.

Compared with the previous relevant results, the main contributions of this paper can be summarized as follows. Firstly, an integrated control law to simultaneously solve the problems of time-varying formation tracking, time-varying delays and switching topologies is proposed in this paper. Secondly, the stability analysis of the close-loop system under the proposed control law is explored with the aid of Lyapunov-Krasovskii function and LMI. Finally, numerical simulations of two task-oriented formation transformation cases, where one is to shape the varying regular hexagon, and the other is to avoid multiple obstacles, are established to verify the effectiveness of the proposed control law.

II. PRELIMINARIES

A. Basic Concepts on Graph Theory

In this paper, the multi-UAV system comprising N UAVs can be regarded as a multi-agent system. Generally, we use a graph denoted by $G = (V, E, A)$ to describe the information exchanges among the UAVs. Denote a single UAV as node

*Research supported by CXJJ-16Z212 and NNSFC No. 61603383.

The authors are all with University of Chinese Academy of Sciences, Beijing 100049 China, and with Institute of Automation, Chinese Academy of Sciences, Beijing 100190 China (e-mail: {xiongtianyi2016, zhiqiang.pu, jianqiang.yi, taoxinlong2104} @ia.ac.cn).

v_i , then $V = \{v_1, v_2, \dots, v_N\}$ is the set of UAVs, and $E \subseteq V \times V$ represents the set of edges, where E is defined such that if $(v_j, v_i) \in E, j \neq i$, there is an edge from UAV j to the UAV i , which means that UAV j can deliver information to UAV i . In addition, $A = [a_{ij}] \in R^{N \times N}$ is the associated adjacency matrix with $a_{ij} \geq 0$. We set $a_{ij} > 0, j \neq i$ if and only if $(v_j, v_i) \in E$; otherwise $a_{ij} = 0$. In this case, UAV j is said to be the neighbor of UAV i if and only if $a_{ij} > 0$, and $N_i = \{v_j \in V : (v_j, v_i) \in E\}$ represents the neighbor set of the i th UAV. A graph is an undirected graph if and only if $a_{ij} = a_{ji}$. Define $D = \text{diag}\{d_1, d_2, \dots, d_N\} \in R^{N \times N}$ as the in-degree matrix, where $d_i = \sum_{v_j \in N_i} a_{ij}$. Then, the Laplacian matrix of graph G is defined as $L = D - A$. A direct path from UAV i to j is a sequence of successive edges in the form of $\{(v_i, v_k), (v_k, v_l), \dots, (v_m, v_j)\}$. Furthermore, an undirected graph is called connected if there is a path between any two UAVs in the graph.

In the case of leader-following, another graph \bar{G} with a virtual leader (labeled as UAV 0) and N UAVs should be considered. The adjacency matrix element associated with the edge from the i th UAV to the virtual leader is denoted by b_i , with $b_i > 0$ if and only if the i th UAV can receive information from the leader.

Note that the interaction topology may dynamically change in reality, so it is necessary to consider all of the possible topologies. Define $\sigma: [0, \infty) \rightarrow P = \{1, 2, \dots, p\}$ as the piecewise constant switching function, where p denotes the number of the possible graphs. Denote $\bar{G}_{\sigma(t)}, a_{ij}(t)$ and $b_i(t)$ as the topology graph at time t , the time varying versions of a_{ij} and b_i , respectively. Consider a finite sequence of non-overlapping bounded and contiguous time intervals $[t_n, t_{n+1})$, $n = 0, 1, 2, \dots$ with $t_0 = 0, 0 < t_{n+1} - t_n \leq T_1, T_1 > 0$. Suppose that in each time interval $[t_n, t_{n+1})$ there exists a sequence of non-overlapping subintervals $[t_n^0, t_n^1), \dots, [t_n^s, t_n^{s+1}), \dots, [t_n^{m_n-1}, t_n^{m_n})$ with $t_n^0 = t_n, t_n^{m_n} = t_{n+1}$ satisfying $t_n^{s+1} - t_n^s \geq T_2 > 0, 0 \leq s \leq m_n - 1$ for some integer $m_n > 0$. Meanwhile, the interaction graph $\bar{G}_{\sigma(t)}$ is supposed to be invariant in each time subinterval $[t_n^s, t_n^{s+1})$, and to switch at time t_n^s . The union graph \bar{G}_{1-m} of a collection of undirected graphs $\bar{G}_1, \bar{G}_2, \dots, \bar{G}_m, m \geq 1$ with the same node set \bar{V} , is a graph with node set \bar{V} and the edge set being the union of the edge sets of graphs $\bar{G}_1, \bar{G}_2, \dots, \bar{G}_m$. Furthermore, the collection of the graphs $\bar{G}_1, \bar{G}_2, \dots, \bar{G}_m$ is called jointly connected if \bar{G}_{1-m} is connected.

Note that the graph \bar{G}_σ in each interval $[t_n^s, t_n^{s+1})$ might not be connected, but have multiple connected subgraphs. Throughout this paper, we suppose that the interaction network is satisfied with the following assumption.

Assumption 1. The collection of the graphs in each interval $[t_n, t_{n+1})$ is jointly connected. Moreover, in each interval $[t_n, t_{n+1})$, there exists at least one UAV having a path to the leader in each connected subgraph.

B. Notations

Throughout this paper, the following notations are used. I_n represents the n dimensional identity matrix; $\bar{\sigma}(\cdot)$ and $\underline{\sigma}(\cdot)$ is the maximum and minimum singular value of a matrix, respectively.

III. PROBLEM DESCRIPTION

In this section, a simplified model of the UAV will be presented first, which can be pre-linearized by adopting feedback linearization. Then, the formation control problem will be described.

A. Model Description

We consider the following simplified model of the i th UAV as follows [6]:

$$\begin{cases} \dot{x}_i(t) = v_i \cos \alpha_i \cos \beta_i, \dot{y}_i(t) = v_i \cos \alpha_i \sin \beta_i \\ \dot{z}_i(t) = v_i \sin \alpha_i, \dot{v}_i = -1/\tau_v (v_i - v_{ci}) \\ \dot{\alpha}_i = -1/\tau_\alpha (\alpha_i - \alpha_{ci}), \dot{\beta}_i = -1/\tau_\beta (\beta_i - \beta_{ci}) \end{cases} \quad (1)$$

where $[x_i, y_i, z_i]^T$ represents the position vector of the i th UAV in 3D space, v_i is the flight velocity, α_i is the flight path angle, and β_i is the heading angle. $v_{ci}, \alpha_{ci}, \beta_{ci}$ are commanded flight velocity, commanded flight path angle, and commanded heading angle, respectively. Moreover, $X_i = [x_i, y_i, z_i, v_i, \alpha_i, \beta_i]^T$ is the state vector of the model for the i th UAV, and $U_i = [v_{ci}, \alpha_{ci}, \beta_{ci}]^T$ is the control input, $i = 1, 2, \dots, N$. $\tau_v, \tau_\alpha, \tau_\beta > 0$ are time constants.

Note that the UAV model (1) is nonlinear. Consequently, input-output feedback linearization method is adopted first, and model (1) can be transformed as follows:

$$\begin{cases} \dot{\bar{x}}_i(t) = \bar{v}_i(t) \\ \bar{v}_i(t) = u_i(t), \end{cases} \quad (2)$$

where $\bar{x}_i = [x_i, y_i, z_i]^T \in R^3$ and $\bar{v}_i(t) = [v_{x_i}, v_{y_i}, v_{z_i}]^T \in R^3$, are the position and the velocity vector of the i th UAV in 3D space, respectively. $u_i = [u_{x_i}, u_{y_i}, u_{z_i}]^T \in R^3$ denotes the auxiliary control input vector of the i th UAV in 3D space, which can be transformed into the actual control input $U_i = [v_{ci}, \alpha_{ci}, \beta_{ci}]^T$ by the following expressions

$$\begin{cases} v_{ci} = (u_{x_i} \cos \alpha_i \cos \beta_i + u_{y_i} \cos \alpha_i \sin \beta_i + u_{z_i} \sin \alpha_i) \tau_v + v_i \\ \alpha_{ci} = (-u_{x_i} \sin \alpha_i \cos \beta_i - u_{y_i} \sin \alpha_i \sin \beta_i) \tau_\alpha / v_i + \alpha_i \\ \beta_{ci} = (-u_{x_i} \sin \beta_i + u_{y_i} \cos \beta_i) \tau_\beta / (v_i \cos \alpha_i) + \beta_i. \end{cases} \quad (3)$$

B. Control Objective

In this paper, we can choose any predefined point or specified UAV as the virtual leader with desired dynamics. Denote the position and velocity of the virtual leader as

$x_0(t) \in R^3$ and $v_0(t) \in R^3$ with $v_0(t) = \dot{x}_0(t)$. In addition, the expected time-varying formation is specified by a command position vector $h_x(t) = [h_{1x}^T(t), h_{2x}^T(t), \dots, h_{Nx}^T(t)]^T$, where $h_{ix}(t) \in R^3$ is a piecewise continuously differentiable vector.

Besides, define $h_v = [h_{1v}^T, h_{2v}^T, \dots, h_{Nv}^T]^T$ with $h_{iv}(t) = \dot{h}_{ix}(t)$.

We define the formation tracking error as $\delta(t) = [\delta_x^T(t), \delta_v^T(t)]^T$, where $\delta_x(t) = [\delta_{1x}^T(t), \dots, \delta_{Nx}^T(t)]^T$ and $\delta_v(t) = [\delta_{1v}^T(t), \dots, \delta_{Nv}^T(t)]^T$ with $\delta_{ix}(t) = \bar{x}_i(t) - x_0(t) - h_{ix}(t)$ and $\delta_{iv}(t) = \bar{v}_i(t) - v_0(t) - h_{iv}(t)$ are position and velocity formation tracking errors, respectively.

Throughout this paper, we consider not only the transfer time delay $\tau_{ij}(t)$ between the i th UAV and the j th UAV, but also the self-delay $\tau_{ii}(t)$ caused by measurement or computation. We suppose that $\tau_{ij}(t)$ and $\tau_{ii}(t)$ are particularly considered as the uniform time delay $\tau_i(t)$, which is generally assumed in the multi-agent consensus control.

We suppose the following assumption naturally holds in this paper.

Assumption 2. $0 \leq \tau_i(t) \leq \tau_m$, $i = 1, 2, \dots, N$ for $t \geq 0$, where τ_m is a positive constant.

Assumption 3: The derivate of the velocity of the virtual leader is bounded, that is, there exists a positive constant v_m such that $\|\underline{f}(t)\| \leq v_m$, where $\underline{f} = [\dot{v}_0^T, \dot{v}_0^T, \dots, \dot{v}_0^T]^T$, $\|\cdot\|$ denotes the Euclidian 2-norm of a vector.

Assumption 4: The derivate of h_v is bounded, that is, there exists a positive constant h_m such that $\|\dot{h}_v\| \leq h_m$, where $\dot{h}_v = [\dot{h}_{1v}^T, \dot{h}_{2v}^T, \dots, \dot{h}_{Nv}^T]^T$.

The control objective of this paper is to design an consensus based formation control law such that the formation tracking error $\delta(t)$ can be rendered small in presence of varying time delays and jointly connected topologies, which leads to a successful time-varying formation tracking for multi-UAV system (1).

IV. FORMATION CONTROL DESIGN AND ANALYSIS

In this section, both formation tracking control law design and stability analysis problems for multi-UAV system (1) with time-varying delays and jointly connected topologies are investigated.

In this paper, it is supposed that only local neighbor information with time delay can be used for the control law design, such that the formation control is fully distributed. Consequently, for the i th UAV, we define local neighborhood tracking position and velocity errors respectively as

$$e_{ix}(t) = \sum_{v_j \in N_i} a_{ij} [\bar{x}_i(t) - h_{ix}(t) - (\bar{x}_j(t) - h_{jx}(t))] + b_i (\bar{x}_i(t) - x_0(t) - h_{ix}(t)) \quad (4)$$

and

$$e_{iv}(t) = \sum_{v_j \in N_i} a_{ij} [\bar{v}_i(t) - h_{iv}(t) - (\bar{v}_j(t) - h_{jv}(t))] + b_i (\bar{v}_i(t) - v_0(t) - h_{iv}(t)). \quad (5)$$

Let $e_x = [e_{1x}^T, e_{2x}^T, \dots, e_{Nx}^T]^T$, $e_v = [e_{1v}^T, e_{2v}^T, \dots, e_{Nv}^T]^T$. Then the system (2) can be written as follows

$$\begin{cases} \dot{e}_x = e_v \\ \dot{e}_v = ((L_\sigma + B_\sigma) \otimes I_3)(u - \underline{f} - \dot{h}_v) \end{cases} \quad (6)$$

where L_σ is the Laplacian matrix of graph $\bar{G}_{\sigma(t)}$ at time t , $B_\sigma = \text{diag}\{b_i\}$, \otimes denotes Kronecker product.

Hence, for the i th UAV, the formation control law is designed as follows:

$$u_i(t) = -k_1 e_{ix} - k_2 e_{iv} + \dot{h}_{iv} \quad (7)$$

where $k_1, k_2 > 0$ are the control gains, e_{ix} , e_{iv} and \dot{h}_{iv} are the short for $e_{ix}(t - \tau_i)$, $e_{iv}(t - \tau_i)$ and $\dot{h}_{iv}(t - \tau_i)$. Then the closed-loop dynamics of the multi-UAV system (2) can be further written as follows under the control law (7):

$$\begin{cases} \dot{e}_x = e_v \\ \dot{e}_v = H_\sigma (-k_1 e_{ix} - k_2 e_{iv} - \underline{f}_0 + \dot{h}_{v\tau} - \dot{h}_v) \end{cases} \quad (8)$$

where $H_\sigma = (L_\sigma + B_\sigma) \otimes I_3$.

Suppose the communication graph \bar{G}_σ on interval $[t_n^s, t_n^{s+1})$ has $l_\sigma \geq 1$ connected subgraphs \bar{G}_σ^j , $j = 1, 2, \dots, l_\sigma$ containing d_σ^j UAVs. The Laplacian matrix of the subgraph \bar{G}_σ^j is denoted by $L_\sigma^j \in R^{d_\sigma^j \times d_\sigma^j}$. Then there exists a permutation matrix $U_\sigma \in R^{N \times N}$ such that

$$(U_\sigma \otimes I_3)^T H_\sigma (U_\sigma \otimes I_3) = \text{diag}\{H_\sigma^1, H_\sigma^2, \dots, H_\sigma^{l_\sigma}\},$$

$$\begin{aligned} e_x^T(U_\sigma \otimes I_3) &= [e_{x\sigma}^{1T}, \dots, e_{x\sigma}^{l_\sigma T}]^T, e_v^T(U_\sigma \otimes I_3) = [e_{v\sigma}^{1T}, \dots, e_{v\sigma}^{l_\sigma T}]^T, \\ e_{x\tau}^T(U_\sigma \otimes I_3) &= [e_{x\tau\sigma}^{1T}, \dots, e_{x\tau\sigma}^{l_\sigma T}]^T, e_{v\tau}^T(U_\sigma \otimes I_3) = [e_{v\tau\sigma}^{1T}, \dots, e_{v\tau\sigma}^{l_\sigma T}]^T, \\ h_v^T(U_\sigma \otimes I_3) &= [h_{v\sigma}^{1T}, \dots, h_{v\sigma}^{l_\sigma T}]^T, h_{v\tau}^T(U_\sigma \otimes I_3) = [h_{v\tau\sigma}^{1T}, \dots, h_{v\tau\sigma}^{l_\sigma T}]^T, \\ \underline{f}^T(U_\sigma \otimes I_3) &= [\underline{f}_{v\sigma}^{1T}, \dots, \underline{f}_{v\sigma}^{l_\sigma T}]^T, \delta^T(U_\sigma \otimes I_6) = [\delta_\sigma^{1T}, \dots, \delta_\sigma^{l_\sigma T}]^T, \\ [\tau_1, \tau_2, \dots, \tau_N]^T U_\sigma &= [\tau_\sigma^1, \tau_\sigma^2, \dots, \tau_\sigma^{l_\sigma}]^T, \end{aligned}$$

where $H_\sigma^j = (L_\sigma^j + B_\sigma^j) \otimes I_3$ with L_σ^j being the Laplacian matrix of corresponding connected subgraph and $B_\sigma^j = \text{diag}\{b_\sigma^j\}$, $b_\sigma^j \in R^{d_\sigma^j}$. $e_{x\sigma}^j = [e_{x\sigma 1}^{jT}, e_{x\sigma 2}^{jT}, \dots, e_{x\sigma d_\sigma^j}^{jT}]^T \in R^{3d_\sigma^j}$, $e_{v\sigma}^j = [e_{v\sigma 1}^{jT}, e_{v\sigma 2}^{jT}, \dots, e_{v\sigma d_\sigma^j}^{jT}]^T \in R^{3d_\sigma^j}$, $\delta_\sigma^j = [\delta_{\sigma 1}^{jT}, \delta_{\sigma 2}^{jT}, \dots, \delta_{\sigma d_\sigma^j}^{jT}]^T \in R^{6d_\sigma^j}$, $\tau_\sigma^j = [\tau_{\sigma 1}^j, \tau_{\sigma 2}^j, \dots, \tau_{\sigma d_\sigma^j}^j]^T \in R^{d_\sigma^j}$, $e_{x\tau\sigma}^j = [e_{x\tau\sigma 1}^{jT}(t - \tau_{\sigma 1}^j), \dots, e_{x\tau\sigma d_\sigma^j}^{jT}(t - \tau_{\sigma d_\sigma^j}^j)]^T$, $e_{v\tau\sigma}^j = [e_{v\tau\sigma 1}^{jT}(t - \tau_{\sigma 1}^j), \dots, e_{v\tau\sigma d_\sigma^j}^{jT}(t - \tau_{\sigma d_\sigma^j}^j)]^T$, $\underline{f}_\sigma^j = [\underline{f}_{\sigma 1}^{jT}, \underline{f}_{\sigma 2}^{jT}, \dots, \underline{f}_{\sigma d_\sigma^j}^{jT}]^T$, $h_{v\sigma}^j = [h_{v\sigma 1}^{jT}, h_{v\sigma 2}^{jT}, \dots, h_{v\sigma d_\sigma^j}^{jT}]^T$, $j = 1, 2, \dots, l_\sigma$.

Then, in each interval $[t_n^s, t_n^{s+1})$, system (8) can be decomposed into the following l_σ subsystems:

$$\begin{cases} \dot{e}_{x\sigma}^j = e_{v\sigma}^j \\ \dot{e}_{v\sigma}^j = H_\sigma^j (-k_1 e_{x\tau\sigma}^j - k_2 e_{v\tau\sigma}^j - \underline{f}_\sigma^j + \dot{h}_{v\tau\sigma}^j - \dot{h}_{v\sigma}^j), j=1, 2, \dots, l_\sigma. \end{cases} \quad (9)$$

The following lemmas play an important role in the proof of the main results.

Lemma 1 [14]. For any real differentiable vector function $y(t) \in R^n$, any differentiable scalar function $\tau(t) \in [0, \tau_0]$ where τ_0 is a positive constant, and any constant matrix $0 < U = U^T \in R^{n \times n}$, we have the following inequality:

$$\begin{aligned} & \tau_0^{-1} [y(t) - y(t - \tau)]^T U [y(t) - y(t - \tau)] \\ & \leq \int_{t-\tau_0}^t \dot{y}^T(\xi) U \dot{y}(\xi) d\xi, t > 0. \end{aligned} \quad (10)$$

Lemma 2 [15]. If the graph is connected, and there are at least one UAV connecting to the leader, then $L_\sigma + B_\sigma$ is positive definite.

Lemma 3 [16]: If the graph is connected, and there are at least one UAV connecting to the leader, then $\|\delta_x\| \leq \|e_x\| / \underline{\sigma}(L_\sigma + B_\sigma)$ and $\|\delta_v\| \leq \|e_v\| / \underline{\sigma}(L_\sigma + B_\sigma)$.

Next, we present the main results of this paper.

Theorem 1. Suppose Assumption 1 holds. Then under the control law (7), time-varying formation for multi-UAV system (1) with time-varying delays and switching topologies can be achieved, if for each connected subgraph in each interval $[t_n^s, t_n^{s+1})$, constants $c_1, c_2, \alpha, \beta, \gamma > 0$ with $\alpha\gamma > \beta^2$ and $k_1, k_2 > 0$ are chosen such that the symmetric matrix $M_\sigma^j > 0$, where

$$M_\sigma^j = \begin{bmatrix} c_1 I & -\frac{1}{2} \gamma I & \frac{1}{2} k_1 \beta H_\sigma^j & \frac{1}{2} k_2 \beta H_\sigma^j \\ -\frac{1}{2} \gamma I & c_2 I - \beta I & \frac{1}{2} k_1 \alpha H_\sigma^j & \frac{1}{2} k_2 \alpha H_\sigma^j \\ \frac{1}{2} k_1 \beta H_\sigma^{jT} & \frac{1}{2} k_1 \alpha H_\sigma^{jT} & c_1 I - c_2 \tau_m^2 k_1^2 & -c_2 k_1 k_2 \tau_m^2 \\ + c_1 I & -c_1 \tau_m^2 I & \times H_\sigma^{jT} H_\sigma^j & \times H_\sigma^{jT} H_\sigma^j \\ \frac{1}{2} k_2 \beta H_\sigma^{jT} & \frac{1}{2} k_2 \alpha H_\sigma^{jT} & -c_2 k_1 k_2 \tau_m^2 & c_2 I - c_2 k_2^2 \tau_m^2 \\ -c_2 I & \times H_\sigma^{jT} H_\sigma^j & \times H_\sigma^{jT} H_\sigma^j & \times H_\sigma^{jT} H_\sigma^j \end{bmatrix}. \quad (11)$$

Proof: Choose the following Lyapunov-Krasovskii functional candidate $V(t) = V_1(t) + V_2(t) + V_3(t)$ with

$$V_1(t) = \frac{1}{2} \alpha e_v^T e_v + \frac{1}{2} \gamma e_x^T e_x + \beta e_x^T e_v \quad (12)$$

$$V_2(t) = c_1 \tau_m \int_{t-\tau_m}^t (\xi - t + \tau_m) \dot{e}_x^T(\xi) \dot{e}_x(\xi) d\xi \quad (13)$$

$$V_3(t) = c_2 \tau_m \int_{t-\tau_m}^t (\xi - t + \tau_m) \dot{e}_v^T(\xi) \dot{e}_v(\xi) d\xi \quad (14)$$

Furthermore, $V_1(t)$, $V_2(t)$, $V_3(t)$ can be rewritten as

$$V_1(t) = \sum_{j=1}^{l_\sigma} \left(\frac{1}{2} \alpha e_{v\sigma}^{jT} e_{v\sigma}^j + \frac{1}{2} \gamma e_{x\sigma}^{jT} e_{x\sigma}^j + \beta e_{x\sigma}^{jT} e_{v\sigma}^j \right) \quad (15)$$

$$V_2(t) = \sum_{j=1}^{l_\sigma} \left(c_1 \tau_m \int_{t-\tau_m}^t (\xi - t + \tau_m) \dot{e}_{x\sigma}^{jT}(\xi) \dot{e}_{x\sigma}^j(\xi) d\xi \right) \quad (16)$$

$$V_3(t) = \sum_{j=1}^{l_\sigma} \left(c_2 \tau_m \int_{t-\tau_m}^t (\xi - t + \tau_m) \dot{e}_{v\sigma}^{jT}(\xi) \dot{e}_{v\sigma}^j(\xi) d\xi \right) \quad (17)$$

Differentiating $V_1(t)$ with respect to t , we can get that

$$\begin{aligned} \dot{V}_1 &= \sum_{j=1}^{l_\sigma} \left((e_{v\sigma}^{jT} \alpha + e_{x\sigma}^{jT} \beta) \dot{e}_{v\sigma}^j + \gamma e_{x\sigma}^{jT} e_{v\sigma}^j + e_{v\sigma}^{jT} \beta e_{x\sigma}^j \right) \\ &= \sum_{j=1}^{l_\sigma} \left((e_{v\sigma}^{jT} \alpha + e_{x\sigma}^{jT} \beta) (H_\sigma^j (-k_1 e_{x\tau\sigma}^j - k_2 e_{v\tau\sigma}^j)) \right. \\ &\quad \left. + (e_{v\sigma}^{jT} \alpha + e_{x\sigma}^{jT} \beta) D_\sigma^j + \gamma e_{x\sigma}^{jT} e_{v\sigma}^j + e_{v\sigma}^{jT} \beta e_{x\sigma}^j \right), \end{aligned} \quad (18)$$

where $D_\sigma^j = -\underline{f}_\sigma^j + \dot{h}_{v\tau\sigma}^j - \dot{h}_{v\sigma}^j$.

Applying Lemma 1, the derivatives of V_2 and V_3 are shown as

$$\begin{aligned} \dot{V}_2 &= \sum_{j=1}^{l_\sigma} \left(c_1 \tau_m^2 \dot{e}_{x\sigma}^{jT}(t) \dot{e}_{x\sigma}^j(t) - c_1 \tau_m \int_{t-\tau_m}^t \dot{e}_{x\sigma}^{jT}(\xi) \dot{e}_{x\sigma}^j(\xi) d\xi \right) \\ &\leq \sum_{j=1}^{l_\sigma} \left(-c_1 (e_{x\tau\sigma}^{jT} - e_{x\sigma}^{jT}) (e_{x\tau\sigma}^j - e_{x\sigma}^j) + c_1 \tau_m^2 e_{v\sigma}^{jT} e_{v\sigma}^j \right) \end{aligned} \quad (19)$$

and

$$\begin{aligned} \dot{V}_3 &= \sum_{j=1}^{l_\sigma} \left(c_2 \tau_m^2 \dot{e}_{v\sigma}^{jT}(t) \dot{e}_{v\sigma}^j(t) - c_2 \tau_m \int_{t-\tau_m}^t \dot{e}_{v\sigma}^{jT}(\xi) \dot{e}_{v\sigma}^j(\xi) d\xi \right) \\ &\leq \sum_{j=1}^{l_\sigma} \left(-c_2 (e_{v\tau\sigma}^{jT} - e_{v\sigma}^{jT}) (e_{v\tau\sigma}^j - e_{v\sigma}^j) + c_2 \tau_m^2 (-k_1 e_{x\tau\sigma}^{jT} \right. \\ &\quad \left. - k_2 e_{v\tau\sigma}^{jT} + D_\sigma^{jT}) H_\sigma^{jT} H_\sigma^j (-k_1 e_{x\tau\sigma}^j - k_2 e_{v\tau\sigma}^j + D_\sigma^j) \right) \end{aligned} \quad (20)$$

where $\eta_\sigma^j = [\bar{\delta}_\sigma^{jT}, \bar{\delta}_{\sigma\tau}^{jT}]^T$.

Combining equations (15)-(20), we have

$$\begin{aligned} \dot{V} &= \dot{V}_1 + \dot{V}_2 + \dot{V}_3 \\ &\leq -z^T M_\sigma^j z + z^T s + \Xi \\ &\leq -\|z\|^2 \underline{\sigma}(M_\sigma^j) + \|z\| \|s\| + \Xi = -V_z(z) \end{aligned} \quad (21)$$

where the matrix M is shown as (11), and $z = [e_{x\sigma}^{jT}, e_{x\tau\sigma}^{jT}, e_{v\sigma}^{jT}, e_{v\tau\sigma}^{jT}]^T$, $s = [\beta D_\sigma^{jT}, \beta D_\sigma^{jT}, -2k_1 c_2 \tau_m^2 H_\sigma^{jT} H_\sigma^j D_\sigma^{jT}, -2k_2 c_2 \tau_m^2 \times H_\sigma^{jT} H_\sigma^j D_\sigma^{jT}]^T$, $\Xi = 2c_2 \tau_m^2 D_\sigma^{jT} H_\sigma^{jT} H_\sigma^j D_\sigma^j$. Under Assumptions 3 and 4, $\|s\|$ and Ξ are bounded.

$V_z(z)$ is positive definite if the matrix M is positive definite and

$$\|z\| \geq \frac{-\|s\| + \sqrt{\|s\|^2 + 4\underline{\sigma}(M)\Xi}}{2\underline{\sigma}(M)}. \quad (22)$$

According to [17], we can draw the conclusion that $z(t)$ is bounded stable. Furthermore, it can be obtained that both $e_{x\sigma}^j$ and $e_{v\sigma}^j$ are bounded stable. Then following Lemma 3, the formation tracking error δ_σ^j is bounded stable in each interval $[t_n^s, t_n^{s+1})$ as $t \rightarrow \infty$. Since the collection of graphs in each interval $[t_n, t_{n+1})$ is jointly connected, it is easy to induce that δ is bounded stable, as $t \rightarrow \infty$ in each interval

$[t_n, t_{n+1})$. That is, δ is bounded stable, as $t \rightarrow \infty$. As a result, we can achieve the expected time-varying formation under time-varying delays and jointly connected topology under the control law (7).

This completes the proof. Next, we discuss the feasibility of $M_\sigma^j > 0$ in Theorem 1.

Remark 1. Evidently, matrix $M_\sigma^j = M_\sigma^{jT}$. It is also obvious that the diagonal elements of the matrix M are positive stable if c_1, c_2, k_1, k_2 are appropriately selected. Therefore, taking τ_m sufficiently small, and choose appropriately choose the values of $c_1, c_2, k_1, k_2, \alpha, \beta$, $M_\sigma^j > 0$ is feasible for each connected subgraph in each interval $[t_n^s, t_{n+1}^{s+1})$. Since the number of the possible interaction graphs is finite, the condition given in Theorem 1 can be always satisfied.

V. SIMULATION

To illustrate the theoretical results obtained in the previous sections, two task-oriented formation transformation cases are simulated, where one is to achieve varying regular hexagon formation, and the other is to avoid multiple obstacles, to verify the effectiveness of the proposed control law.

Consider a multi-UAV system with six UAVs where the dynamics of each UAV are described by (1). In addition, the virtual leader is set as the formation center.

To verify the effectiveness of the proposed control law, in the following two cases, choose the interaction graphs as $\{\bar{G}_1, \bar{G}_2, \bar{G}_3\}$ which are shown in Fig. 1, and the union graph \bar{G}_{1-3} of graphs $\bar{G}_1, \bar{G}_2, \bar{G}_3$ is also depicted in Fig. 1. Assume that the communication graphs switch in the following order: $\bar{G}_1 \rightarrow \bar{G}_2 \rightarrow \bar{G}_3 \rightarrow \bar{G}_1 \dots$, and each graph stays active for 0.1s which conforms to reality. Such a scenario is to some extent really challenging since there are only a few communication links available at any time, which subsequently extends the control period of a complete loop. Moreover, it can be seen from Fig. 1 that the graphs $\bar{G}_1, \bar{G}_2, \bar{G}_3$ are jointly connected, and for each connected subgraph, there exists a UAV receiving information from the leader, which implies that Assumption 1 is satisfied.

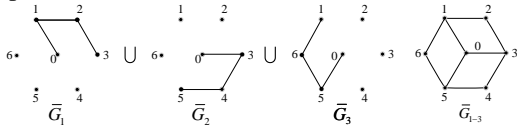


Figure 1. Possible interaction graphs and the union graph.

Besides, the different varying time delays are set as $\tau_1 = \tau_3 = 0.03 + 0.02\sin(0.1t)$, $\tau_2 = \tau_4 = 0.04 + 0.01\sin(0.1t)$, $\tau_5 = \tau_6 = 0.04 + 0.02\sin(0.1t)$. In addition, Choose the same control gains in control law (7) as $k_1 = 1, k_2 = 3$.

Case I: Shaping varying regular hexagon formation.

In this case, the six UAVs are supposed to keep a parallel

hexagon formation at the same height and at the same time to keep rotating around the virtual leader whose trajectory is expressed by $x_0(t) = [5t, 5t, 5t]^T$. Thus, the time-varying formation is specified by

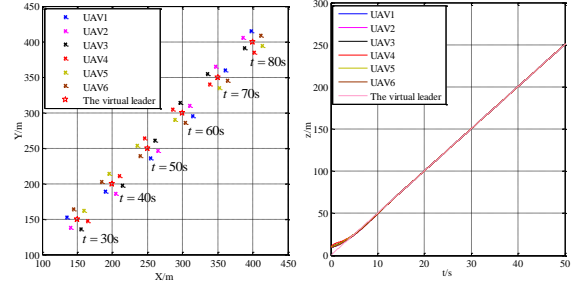
$$h_{ix}(t) = \begin{bmatrix} 15\cos(0.1t + (i-1)\pi/3) \\ 15\sin(0.1t + (i-1)\pi/3) \\ 0 \end{bmatrix}, i = 1, 2, \dots, 6.$$

In addition, the initial states are shown in Table I.

TABLE I. THE INITIAL POSITIONS AND VELOCITIES OF SIX UAVS

Initial states	UAV					
	UAV1	UAV2	UAV3	UAV4	UAV5	UAV6
$[x_i(0), y_i(0), z_i(0)]$	[-20, 10, 10]	[20, -20, 10]	[-20, 20, 10]	[15, 15, 15]	[-20, -15, 10]	[-15, -10, 10]
$[v_i(0), \alpha_i(0), \beta_i(0)]$	[5, 4, 45]	[5, 4, 45]	[5, 5, 40]	[5, 1, 60]	[5, 4, 45]	[5, 4, 45]

The simulation results are shown in Figs. 2-3. Fig. 2(a) displays the positions of the six UAVs and the virtual leader at $t=30s, 40s, 50s, 60s, 70s, 80s$ in X-Y plane, and Fig. 2(b) shows the time histories of the height of the six UAVs and the virtual leader, and Fig. 3 depicts the formation position tracking errors on X-axis, Y-axis and Z-axis.



(a). Position snapshots of the six UAVs and the virtual leader. (b) The trajectories of the height of the six UAVs and the virtual leader.

Figure 2. Position snapshots and the trajectories of the height of the six UAVs and the virtual leader.

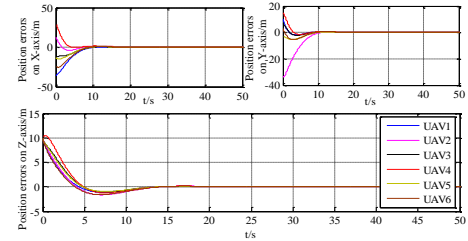


Figure 3. Formation position tracking errors on X-axis, Y-axis and Z-axis.

From Figs. 2, the following phenomena can be observed: (i) the six UAVs successfully keep a parallel hexagon formation in X-Y plane even though there exist time delays and the topologies are changing; (ii) the parallel hexagon keeps rotation around the virtual leader; (iii) the virtual leader moves along a straight line, and keeps lying in the center of the formation, so that the formation moves along the same straight line in X-Y plane; (iv) the six UAVs keep flying at the same varying altitude as the leader. From Fig. 3, it can be seen that the formation position tracking errors converge to around 0 at $t=20s$, and the response time is a bit long which is reasonable because the initial positions are too far and the topology does not keep connected all the time and the

information sharing among UAVs exists delays as well.

Case 2: Formation transformation to avoid obstacles

On various occasions, the formation needs to make corresponding adjustment when encountering obstacles or needing larger sensing coverage. In this case, the leader is supposed to track the trajectory expressed by $x_0(t)=[5t, 0, 100]^T$. In addition, we assume that the six UAVs firstly keep a column formation at a height of 100 meters in which the distance between any two adjacent UAVs is 6 meters, and then enlarge the distance to avoid three obstacles, lastly the UAVs also keep the column formation in which the distance between any two adjacent UAVs is 16 meters as expected. Fig. 4 illustrates the motion trajectories of the six UAVs and the positions of the obstacles. Thus, the time-varying formation can be specified by

$$h_x(t)=[f_{1x}(t), f_{1y}(t), f_{1z}(t), \dots, f_{N_x}(t), f_{N_y}(t), f_{N_z}(t)]^T, \quad (23)$$

$$\text{where } f_{ix}(t) = f_{iz}(t) = 0, \quad f_{iy}(t) = \begin{cases} 15, & 0s \leq t \leq 20s \\ 35, & 20 < t \leq 60s \\ 40, & 60s < t < 100s \end{cases}, \quad \text{and}$$

according to Fig. 4, in the same way, we can get $f_{iy}(t)$, $i \geq 2$. In addition, to generate a smoother transient process for formation transformation and a more realizable command, the original formation vector command $h_x(t)$ needs to be processed through a command processor by adopting nonlinear tracking differentiator (NTD) technique [18].

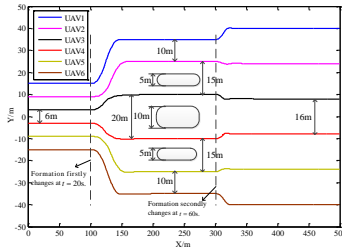


Figure 4. The motion trajectories of the UAVs.

In Fig. 4, it can be observed that the three predefined formations are successfully achieved by adopting the proposed control law. Besides, the formation varies due to three obstacles at $t=20s$ for the first time and changes again at $t=60s$ as expected. During the two processes of formation alternation, the trajectories are also very smooth, which can prevent UAVs in some extent from crashing with each other.

Therefore, the two cases demonstrate the validity and effectiveness of the proposed control law.

VI. CONCLUSION

In comparison with time-invariant formation, time-varying formation is obviously more practical in many applications. For the purpose of achieving expected time-varying formation under time-varying delays and jointly connected topologies, we design a consensus based control law. Based on graph theory, the stability of the close-loop system with the proposed control law is analyzed by applying Lyapunov-Krasovskii function and LMI. Numerical simulation results

of two task-oriented cases illustrate the validity and effectiveness of the obtained theoretical results. Future research directions include extending the results in this paper to the case where the condition of communication network is more general, such as directed topologies.

REFERENCES

- [1] A. K. Das, R. Fierro, V. Kumar, J. P. Ostrowski, J. Spletzer and C. J. Taylor, "A vision-based formation control framework," *IEEE Transactions on Robotics and Automation*, vol. 18, no. 5, pp. 813-825, 2002.
- [2] T. Balch and R.C. Arkin, "Behavior-based formation control for multi robot teams," *IEEE Transactions on Robotics and Automation*, vol. 14, no. 6, pp. 926-939, 1998.
- [3] M. A. Lewis and K. Tan, "High precision formation control of mobile robots using virtual structures," *Autonomous Robots*, vol. 4, 387-403, 1997.
- [4] T. Xiong, Z. Pu and J. Yi, "Time-varying formation finite-time tracking control for multi-UAV systems under jointly connected topologies," *International Journal of Intelligent Computing and Cybernetics*, vol. 10, no. 4, pp. 478-490, 2017.
- [5] M. Ou, H. Du and S. Li, "Finite-time formation control of multiple nonholonomic mobile robots," *International Journal of Robust and Nonlinear Control*, vol. 24, no.1, pp. 140-165, 2014.
- [6] R. Xue, J. Song, and G. Cai, "Distributed formation flight control of multi-UAV system with nonuniform time-delays and jointly connected topologies," *Proceedings of the Institution of Mechanical Engineers Part G:Journal of Aerospace Engineering*, vol. 230, no. 10, pp. 1871-1881, 2016.
- [7] M. Ge, Z. Guan, C. YANG, T. Li and Y. Wang, "Time-varying formation tracking of multiple manipulators via distributed finite-time control," *Neurocomputing*, vol. 202, pp. 20-26, 2016.
- [8] X. Dong, Y. Zhou, Z. Ren and Y. Zhong, "Time-varying formation tracking for second-order multi-agent systems subjected to switching topologies with application to quadrotor formation flying," *IEEE Transactions on Industrial Electronics*, vol. 64, no. 6, pp. 5014-5024, 2017.
- [9] H. Xia, T. Huang, J. Shao and J. Yu, "Leader-following formation control for second-order multi-agent systems with time-varying delays," *Transactions of the Institute of Measurement and Control*, vol. 36, no. 5, pp. 627-636, 2014.
- [10] Z. Yan, Y. Liu, C. Liu and J. Zhou, "Leader-following coordination of multiple UAVs formation under two independent topologies and time-varying delays," *Journal of Central South University*, vol. 24, no. 2, pp. 382-393, 2017.
- [11] X. Dong and G. Hu, "Time-varying formation control for general linear multi-agent systems with switching directed topologies," *Automatica*, vol. 73, no. C, pp. 47-55, 2016.
- [12] X. Dong, Y. Zhou, Z. Ren and Y. Zhong, "Time-varying formation control for unmanned aerial vehicles with switching interaction topologies," *Control Engineering Practice*, vol. 46, pp. 26-36, 2016.
- [13] P. Li, K. Qin and H. Pu, "Distributed robust time-varying formation control for multiple unmanned aerial vehicles systems with time-delay," *29th Control and decision Conference*, Chongqing, China, pp. 1539-1544, 2017.
- [14] Y. Sun, L. Wang and G. Xie, "Average consensus in networks of dynamic agents with switching topologies and multiple time-varying delays," *Systems and Control Letters*, vol. 57, no.2, pp. 175-183, 2008.
- [15] F. Wang, H. Yang, Z. Liu and Z. Chen, "Containment control of leader-following multi-agent systems with jointly-connected topologies and time-varying delays," *Neurocomputing*, vol. 260, no.18, pp. 341-348, 2017.
- [16] H. Zhang and F. Lewis, "Adaptive cooperative tracking control of higher-order nonlinear systems with unknown dynamics," *Automatica*, vol. 46, no. 7, pp.1432-1439, 2012.
- [17] H. Khalil, *Nonlinear Systems*, 3rd ed. Pearson Education, 2002, pp.168-174.
- [18] J. Q. Han, "From PID to active disturbance rejection control," *IEEE Transactions on Industrial Electronics*, vol. 56, no. 3, pp. 26-36, 2009.